Effect of Heat Treatment on the Molecular and Functional Properties of Pea Protein Isolate

Food Biophysics (2025) 20:64
https://doi.org/10.1007/s11483-025-09954-x

RESEARCH

Effect of Heat Treatment on the Molecular and Functional Properties of Pea Protein Isolate

Rui Liu[1,2] · Camilla P. Frederiksen[3] · Trine R. Rasmussen[3] · Serafim Bakalis[3] · Poul Erik Jensen[3] · Svemir Rudić[4] · Heloisa N. Bordallo[1] · Ourania Gouseti[3]

Received: 26 November 2024 / Accepted: 13 March 2025

Abstract
This work aimed at understanding the effect of heat treatment on the properties and functionalities of pea protein isolate (PPI). PPI was characterised using thermogravimetric methods coupled with evolved gas analysis, differential scanning calorimetry, and X-Ray powder diffraction. As water is an integral component in determining protein properties, inelastic neutron scattering was further used to study water populations in the PPI powder. Hydration time was identified as key in determining solubility. Heat treatment resulted in partially denatured, more soluble, less thermodynamically stable, and less crystalline PPI compared to the control. Heating, often associated with protein aggregation and particle size increase, was found to reduce PPI particle sizes, which was attributed to the disruption of non-covalent interactions. During emulsification, these features enhanced formation of smaller drops, stable against coalescence. Compared to the control, the heat-treated PPI produced emulsions with increased shear thinning (power law index of 0.6 compared to 0.9) and consistency (≈10 times higher), as it has been previously reported for emulsions with fine, compared to coarse, droplets. Acid-induced gels of the heat-treated PPI were ≈4 times more elastic (G') compared to the control. Overall, this work contributes towards the design of plant-based foods with predictable characteristics by understanding the link between protein physicochemical properties and food functionality.

Keywords Pea protein isolate · Heat-treatment · Protein functionality · Inelastic neutron scattering · Food analogues · Plant protein

Introduction

Although a good source of readily bioavailable protein, high consumption of animal-based foods has recently been associated with important environmental challenges (e.g., livestock is responsible for about 15% of the total anthropogenic greenhouse gas emissions [1]), adverse health effects (e.g., increased risk for obesity and type-2 diabetes [2]), and animal welfare concerns. Interest in plant-based proteins is therefore increasing rapidly. Yellow peas can contain up to 25% protein, making them an excellent candidate for the transition to more plant-based diets [3].

Globulins make about 80% of the pea storage proteins. The two main globulin types are the 11S (legumin) and 7S (vicillin and convicillin). Legumins are proteins with hexameric quaternary structure comprising six nearly identical subunits of molecular weight ≈60 kDa. Each subunit contains an acidic (α-legumin, ≈40 kDa) and a basic (β-legumin, ≈20 kDa) polypeptide chain, which are linked together with a disulphide bridge. Vicillin and convicillin both have trimeric structures, with molecular weights of about 170 kDa and 290 kDa, respectively [4].

Storage proteins are densely packed in protein bodies within the seed cells, and they can be extracted using methods based on wet fractionation to produce protein isolates [5]. During wet fractionation, globulins are first solubilised at alkaline pH values (i.e., away from their isoelectric point

✉ Ourania Gouseti
ourania@food.ku.dk

1 Niels Bohr Institute, University of Copenhagen, Copenhagen, Denmark

2 Department of Chemistry and Chemical Engineering, Chalmers University of Technology, Gothenburg, Sweden

3 Department of Food Science, University of Copenhagen, Copenhagen, Denmark

4 ISIS Facility, STFC, Rutherf
ord Appleton Laboratory, Chilton, Didcot OX11 0QX, UK

Published online: 31 March 2025

(pI)), they are separated from the non-soluble material, and they are then precipitated by lowering the pH close to their pI. The globulin-rich pellets are finally neutralised to pH 7 and spray dried to produce the powder isolate [5]. This process can cause changes in the molecular conformation of the proteins, and it can produce large, insoluble protein aggregates [6, 7]. Compared to animal proteins, pea protein isolates (PPI) present inferior functional properties, partly due to their poor solubility and the formation of insoluble aggregates during protein extraction [8]. By improving the way food products are manufactured one can ensure their optimal quality and safety[9–13].

It is well established that, among other factors, hydration can be key in determining protein properties, for example it can govern protein conformation, solubility, and stability through mediating long-range interactions between polar and charged amino acids, particularly for large and multidomain protein molecules and aggregates as found in PPI [14]. At low moisture contents, water can act as a plasticiser, providing mechanical softness and molecular mobility upon hydration [15, 16]. Protein-water interactions have therefore been investigated for the development of plant-based analogues including dairy and meat alternatives [17, 18].

Heating can affect non-covalent interactions such as hydrogen bonds, salt bridges, and hydrophobic interactions that keep protein aggregates connected, and protein molecules folded. As a result, aggregates may break, and protein molecules may unfold [19, 20]. Protein unfolding may further expose previously hidden hydrophobic regions, thus promoting new hydrophobic interactions and formation of new protein–protein aggregates. Heat treatment is therefore often associated with particle size increase in proteins [20, 21].

Understanding the link between molecular interactions and food protein functionality can enhance predictable novel food design[22]. For pea protein, unfolding has previously associated with improved solubility and emulsifying properties, which was attributed to enhanced flexibility and film-forming potential[23].

Within the past 15 years, neutron scattering has been identified as a powerful tool with potential applications for plant-based food materials [24]. Inelastic neutron scattering (INS) is a non-invasive technique that can provide information about the motion of the atoms within the molecule, including interactions with water [25]. INS data can be used to acquire information regarding changes within the molecule, such as oxidation or breakage of disulphide bridges, a conversion that is difficult to observe using infrared or Raman spectroscopy. Use of INS in food research is therefore relevant.

To date, milk proteins are among the most studied protein ingredients [26], followed by soy proteins. The present work studies the effect of heating on PPI, focusing on a range of length scales, from molecular to micro scale, with the aim to link physicochemical properties with food functionality. First, non-heated and heated ingredients were characterised, including water interactions, thermal properties, and structural ordering. Then, their emulsifying and gelling functionalities were linked with their ingredient attributes.

Materials & Methods

Materials

Pea protein isolate (Pisane™, C9, lot 2,020,270,456; 81.7% protein, 0.7% carbohydrates, 9% fat, 5% salts) was supplied by Cosucra (Warcoing, Belgium). Rapeseed oil (Ollineo) was purchased from a local supermarket. D-(+)-Gluconic acid delta-lactone (GDL) was purchased from Sigma (Lot # SLCF 8971). Fast Green (F.C.F.) and Nile red were obtained from BioGnost® (Croatia) and Invitrogen™ (USA), respectively. Demineralised water was used.

Methods

Preparation of Control and Heat-Treated PPI

30 mL of 10% (w/v) pea protein isolate (PPI) dispersions were prepared (vortex) and left to hydrate (for 0.5 h or 20 h) in a rotating device (Grant-bio Mini rotator PTR-25, Kisker Biotech, Germany) at 32 rpm, room temperature. Samples for heat treatment were then heated in a shaking water bath (LSB Aqua Pro Linear Shaking Water bath, using shaking of 125 rpm) at 90 °C for 30 min, after which they were left to cool to room temperature. Control (i.e., not heat-treated) and heat-treated samples were either used to prepare and characterise emulsions and gels (Sects. "Preparation of emulsions and gels"-"Visualisation") or freeze-dried (48 h) and the resulting powder was characterised (Sects. "Effect of hydration time"-"Inelastic Neutron Scattering").

Effect of Hydration Time

First, the effect of hydration time on the solubility of control (i.e., not heated) and heat-treated PPI was measured for proteins that were hydrated for 6 h and for 20 h, by determining the protein content of the supernatant after centrifugation (4000 g, 30 min, 25 °C, Sigma 3K15 Refrigerated Centrifuge) using the Bradford method (100 µL of sample were mixed with 5 mL of diluted (1:4 with Milli-Q water) Bradford reagent, the mixture was left to react for 5 min, absorbance measured at 595 nm (UV-1280 spectrophotometer, Shimadzu, Denmark), BSA used as standard for the calibration curve), and dividing it with the total amount of protein (calculated using the manufacturer's declaration for

protein content in the PPI). Despite the reported limitations of the Bradford assay [27], the method was selected due to its simplicity and the absence of surfactants in the samples. It is anticipated that potential errors would be systematic and would therefore allow ranking of the solubility in the different preparations as seen in Sect. "Selecting hydration time".

To further understand the effect of hydration on the PPI, the freeze-dried material was left to equilibrate for 1 week in either 20% or 85% relative humidity (RH) vacuum tidely desiccators at 24 °C (no microbial growth was evidenced), and it was analysed using thermal gravimetric analysis (TGA) and Differential Scanning Calorimetry (DSC), as described in Sects. "Evolved gas analysis: TGA-FTIR" and "Differential Scanning Calorimetry", respectively.

Evolved Gas Analysis: TGA-FTIR

TGA was conducted using a Netzsch TG 209 F1 Libra (Netzsch, Germany) apparatus, simultaneously coupled with a Bruker Fourier transform infrared (FTIR) spectrometer. Data were analysed using the Proteus software (Bruker, Germany) equipped with an automatic sample changer. Samples were added to clean alumina crucibles and lightly pressed. Gas flow of 20 ml/min protective N_2 and 20 ml/min purge N_2 was used. Samples were heated from 20 °C to 220 °C (at 10 °C/min) as this was deemed a safe temperature range where the samples would not contaminate the instrument, while still allowing for detection of the onset of thermal degradation. Sample mass of under 5 mg was used, measured to µg precision. Absorption FTIR spectra were collected every 3 min in the spectral range 650–4400 cm^{-1}.

Differential Scanning Calorimetry

DSC data were taken with a Netzsch 214 Polyma and analysed using Proteus software. Aluminium crucibles with punched lids were used. Crucibles and samples were weighed at mg precision. Gas flow 40 ml/min protective N_2 and 60 ml/min purge N_2 was used. Samples were left at 30 °C (15 min), then heated (10 °C/min) to 200 °C. Liquid N_2 was used to stabilise temperature.

X-Ray Powder Diffraction (XRPD)

XRPD data were acquired with a Bruker D8 Discover diffractometer. Samples were placed into PMMA sample holders and patted flat. Each sample was measured over two hours with wavelength 1.5406 Å (Cu Kα) in the range 5–50° at room temperature. Relative crystallinity (RC), defined as the ratio of the crystalline area to the total diffraction area, was determined using Eq. (1).

$$RC(\%) = \frac{A_c}{A_c + A_a} \times 100 \quad (1)$$

where A_c is the crystalline area and A_a is the amorphous area in the XRPD diffractogram.

Inelastic Neutron Scattering

Information on molecular vibrations occurring over an energy range from 50 to 4000 cm^{-1}, corresponding to the femtosecond, time domain, was obtained using the indirect geometry time-of-flight neutron spectrometer TOSCA [28], at ISIS Facility, UK. Spectra were recorded below 20 K. Sample was confined in a flat aluminium container sealed with indium wire. Data were converted to the incoherent dynamic structure factor, S(Q, ω), using Mantid [29]. The data were normalised to the intensity of the elastic line and compared to the spectra of ice.

Preparation of Emulsions and Gels

To prepare emulsions and gels, control and heat-treated samples were first homogenised for 2 min at 9500 rpm using Ultra Turrax (T-25, Janke & Kinkel, IKA labortechnik, Germany). For the emulsions, 10% of rapeseed oil was added (i.e., 10% of the sum weight of the water and protein), and samples were emulsified with Ultra Turrax (4 min, 13,500 rpm). For the gels, 2% GDL was then added in the emulsions, and the mixture was shaken for 10 s by hand, transferred immediately to petri dishes, and left to set at room temperature overnight. A workflow diagram that details the relevant analyses performed is shown in Fig. 1a. As acidification rate and extend with GDL depends on the exact concentration, preliminary experiments were carried out to achieve the desired acidification curve (shown in Fig. 1b).

Particle Sizes

Particle sizes were measured with Mastersizer 3000 Hydro MV (Malvern Panalytical, UK) using the process described by Masiá et al. [30] with minor modifications. For systems without oil, refractive index was 1.52, absorption index 0.001, density 0.919 g/cm^3, water as dispersant with refractive index of 1.334, stirring speed 2400 rpm. For systems with oil, refractive index was 1.465, density 0.915 g/cm^3, water as dispersant, stirring speed 500 rpm. Particle sizes were measured in duplicates.

Emulsion Stability

Emulsion stability was measured using a similar procedure as in [30] by pipetting 5 mL sample to a flat-bottomed

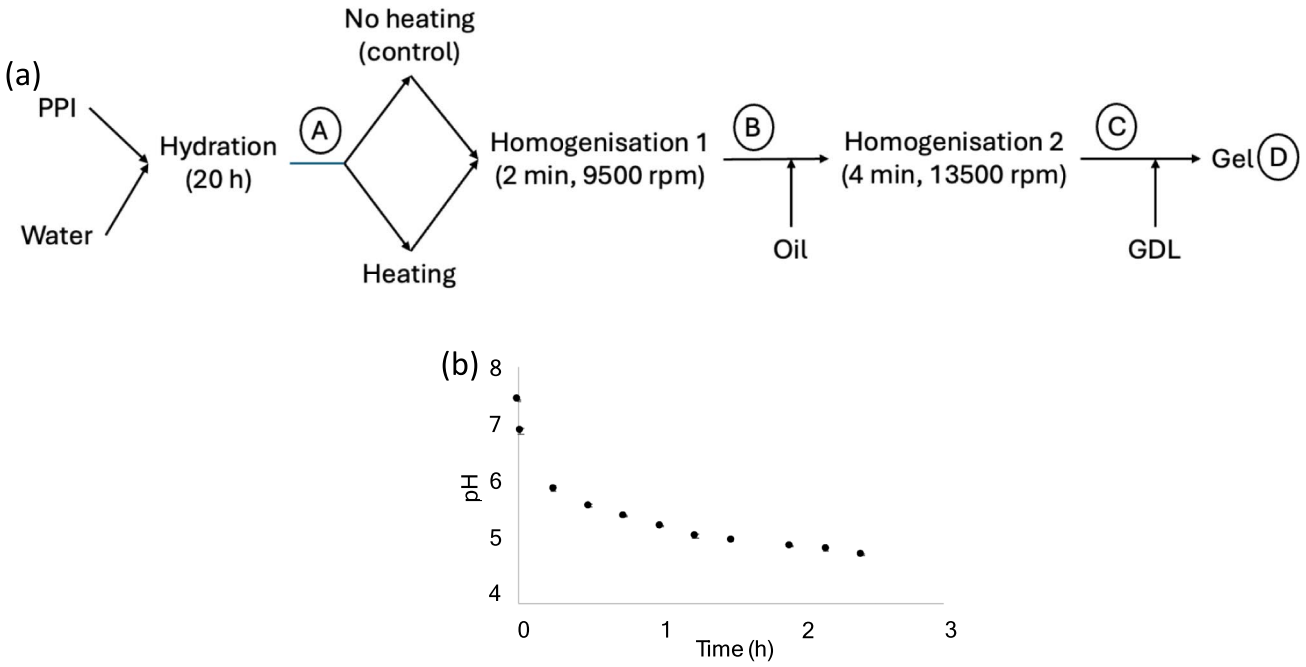

Fig. 1 (**a**) Workflow diagram (samples from points A, B, and C were analysed for particle size and zeta potential; samples from point C were further examined for microstructure, emulsion stability, and viscosity; samples from point D were evaluated for microstructure and rheology); (**b**) acidification curve during gelation with 2% GDL. Averages of triplicates with one standard deviation as error bars are shown

cylindrical glass cell and measuring backscattering (initial sample height: 55 mm) with Turbiscan MA 2000 (C.R.Hintze ApS, Sweden) at 20 °C, and times 0, 3 h, 2 days, 3 days, and 7 days, while stored at room temperature. Measurements were performed in duplicates.

Zeta Potential

Zeta potential of diluted (with Milli Q water) control and heat-treated samples was measured using a Malvern Zetasizer Nano-ZSP (Malvern Panalytical, Malvern, UK) in duplicates using the procedure of [30].

Rheology

Rheology of emulsions and gels was measured with a Kinexus Pro (Netzxch, Selb, Germany). Viscosity of emulsions was measured in duplicates with cone-plate geometry, shear ramp of 0.1–100 s^{-1}, logarithmic change of shears, ramp time 10 min, 10 samples per decade. Viscoelastic properties of gels were evaluated with an amplitude sweep test at 1 Hz, strain 0.10–500%, logarithmic strain change step, 10 samples per decade, run time 20 min. Experiments were carried out at 25 °C in biological duplicates. As differences were < 5%, single measurements are shown in the results and discussion section. Viscosity results were fitted to the power-law model as described with Eq. 2 [31], and the power-law index and consistency are reported.

$$\sigma = \mathrm{K} \bullet \dot{\gamma}^{n} \tag{2}$$

where σ is the shear stress, K the consistency, $\dot{\gamma}$ the shear rate, and n the power-law index.

Visualisation

Macrostructure was captured with an iPhone camera. Microstructure was visualised with a Stellaris 5 confocal laser scanning microscope (CLSM, Leica Microsystems, US), 66 × lens following a procedure similar to [32]. 1–2 µL of sample were placed on a 10-well glass slide and mixed (manually) with Nile red (emission 560–580 nm, excitation 488 nm) and Fast Green (emission at 650–680 nm, excitation at 633 nm) to stain the lipids and proteins, respectively. Lipids appeared green, and proteins red. Representative images are shown in Fig. 7.

Statistics

Where relevant, results are presented as means with error bars showing one standard deviation. One-way ANOVA (analysis of variance) was performed to evaluate significant

differences, verified with Tukey's HSD (honestly significant difference) test. Significant differences were assumed at 95% confidence intervals ($P < 0.05$), as in [32]. The neutron scattering experiments are based on counting, and the presented results were obtained after 4 h of data collection for each sample allowing for an optimal fractional error bar as defined by Poisson statistics.

Results & Discussion

Selecting Hydration Time

Solubility of PPI that has been hydrated for 30 min or 20 h (overnight) without heating (control) and with subsequent heating at 90 °C and cooling (heat-treated) was tested to select appropriate conditions for the subsequent experiments. In both control and heat-treated systems, solubility increased (by 190% and 115%, respectively) when PPI was pre-hydrated for 20 h, compared to 30 min (Fig. 2), any additional time had less influence (data not shown).

To better understand the effect of hydration on the behaviour of PPI, the material was equilibrated for 7 days in low (20%) and high (85%) RH. Hydration was confirmed by 20% weight difference between the two conditions, normalised to the same initial weight. TGA curves (Fig. 3a) show two events of mass loss for both samples, one with maximum rate at temperatures < 100 °C and one with onset temperature > 160 °C and peak temperature > 220 °C (where the experiment was stopped). The first loss at T < 100 °C is attributed to water evaporation, and the relevant maximum peak temperature, referred to as dehydration temperature T_{dehydr}, was determined by the dTGA curves at 80 °C and 70 °C for the samples at 20% and 85% RH, respectively. The shift in T_{dehydr} towards lower values on increasing hydration indicates weaker binding of bulk water with the protein [33]. The second mass loss is attributed to protein degradation,

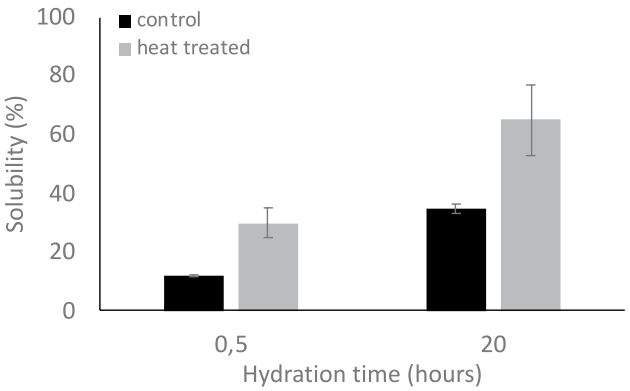

Fig. 2 Solubility of pea protein isolate pre-hydrated for 30 min and 20 h without heating (control) or after heating at 90 °C (heat-treated)

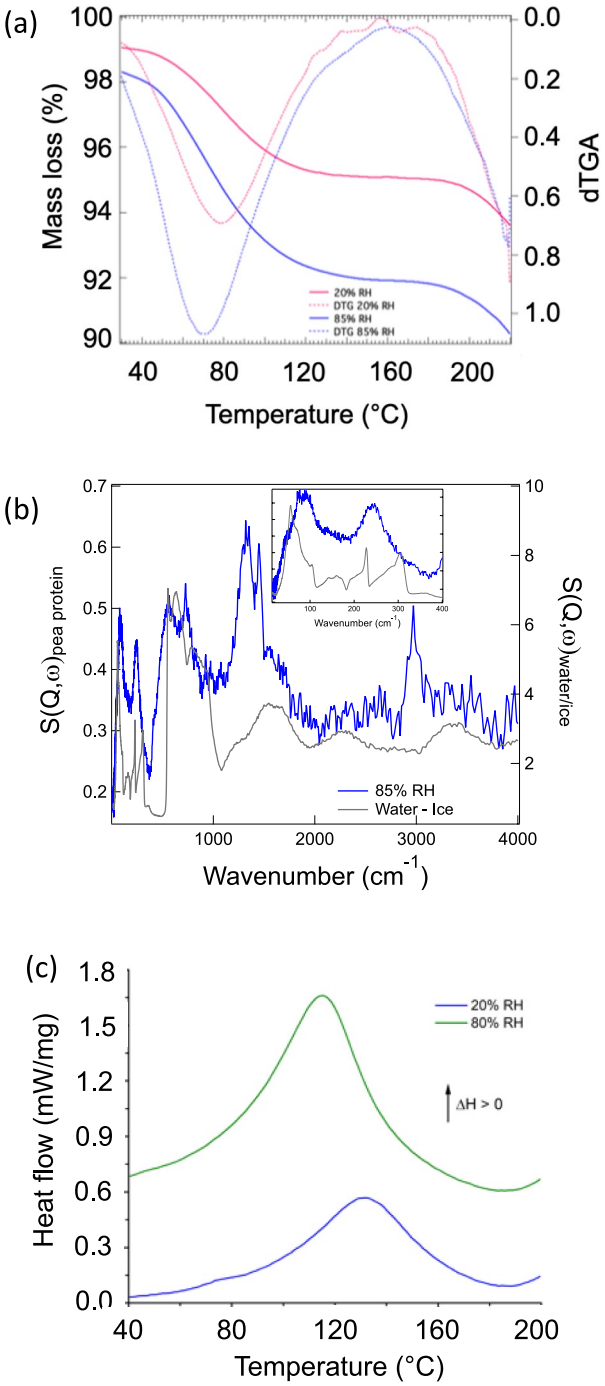

Fig. 3 Properties of samples at low (20%) and high (85%) relative humidity: (**a**) TGA and dTGA curves at heating rate 10 K/min; (**b**) Inelastic Neutron Scattering spectra (data for the sample at 85% RH are compared with the water spectrum), the inlet shows magnification of the curves for 15–400 cm^{-1}; (**c**) DSC heating curves at 10 K/min

with results indicating lower onset temperature, therefore less thermostable sample, at higher hydration levels. At 220 °C, the sample at low and high hydration had lost 5.5% and 8% of their initial mass, respectively, the difference

largely caused by the different water contents. Water dynamics of the 85% RH sample were further studied by comparing its INS spectrum to that of pure water (Fig. 3b). A sharp peak at 72 cm^{-1} is observed (inset). Knowing that bulk water is characterised by a sharp excitation around 50 cm^{-1}, while confined water molecules are described by a vibrational mode centred at about 80 cm^{-1}, the observation of the sharp peak at 72 cm^{-1} confirms the presence of coordinated water, likely related to a hydration layer. The broad shoulder around 50 cm^{-1} further confirms the presence of bulk water, while the features between around 550 cm^{-1} confirm the presence of non-coordinated water.

DSC data (Fig. 3c, Table 1) show a peak with maximum at 100 °C < T < 140 °C. According to the TGA results, this transition occurs after the first bulk water evaporation (T_{dehydr} < 100 °C) and before protein degradation (T_{degrad} > 140 °C), although correlation between the two techniques is indirect as the experimental conditions are not identical (e.g., open and pinched crucibles in TGA and DSC, respectively). This peak is attributed to protein denaturation, with the denaturation temperature, T_{denat}, referring to the temperature at the maximum peak height. The denaturation curves show some interesting features. Firstly, T_{denat} decreased and the associated enthalpy change increased with increasing hydration. This was expected, as denaturation requires a certain degree of water [34]. Comparable T_{denat} (> 100 °C) have previously been reported for soybean protein at similar moisture contents [35]. Secondly, the curve at low RH is more asymmetric compared to that at high RH. This has previously been related to the reversibility of the process, with asymmetric peaks linked to more irreversible protein denaturation [34]. Similar to Fig. 3c, the authors reported higher asymmetry and reduced reversibility for lysozyme denaturation at lower moisture contents [34]. Thirdly, a small shoulder is noticeable at about 75 °C for the curve at 20%RH. This was persistent for all systems at low moisture content, and it was also evident in the DSC heating curves of lysozyme at RH < 60% [34], however the authors did not comment upon it. It is speculated that this shoulder may be related to glass transition of the protein. While proteins in solution have negative glass transition temperatures (T_g), onset T_g up to 120 °C has been reported for β-casein at low water activities [36].

Overall, increased hydration levels appeared to increase protein solubility by ways that may include enhanced water mobility and increased protein interactions with water. Hydration of 20 h (overnight) was therefore selected for the remaining of the experiments.

Table 1 Thermal analysis data of the samples at low (20%) and high (85%) relative humidity (RH)

Sample	Mass loss at 220 °C (%)	T_{dehydr} (°C)	T_g (°C)	T_{denat} (°C)	ΔH (J/g)
20% RH	5.5	80	74 ± 1	126 ± 7	137 ± 19
85% RH	8	70	n/a	119 ± 6	317 ± 34

Effect of Heat Treatment on the Physicochemical Properties of PPI

TGA data of the untreated (as received), control (hydrated and freeze-dried), and heat-treated (hydrated, heated, and freeze-dried) PPI confirmed two mass loss events, one with maximum rate at T < 100 °C, and one with onset T > 175 °C for all three samples (Fig. 4). Oxidation was not evident when samples were heated under O_2 (curves similar to those in Fig. 4, data not shown for simplicity). At T < 100 °C, evolved gas FTIR spectra displayed the characteristic peaks of water, suggesting water evaporation as the main contributor to the mass loss. However, due to the complexity of the sample and the PPI preparation conditions (the protein is extracted chemically from the pea seed and spray-dried to high temperatures to produce the powder), contributions from small amounts of volatile compounds with spectra that overlap to that of water cannot be ruled out. For example, Xiang et al. have characterised 51 volatile compounds in PPI, including aldehydes, ketones, acids, alkanes esters, furans, phenol [37]. The degree of hydration, evaluated as the mass lost at 170 °C (Table 2), was higher (by up to 20%) for the untreated compared to the control and heat-treated samples, possibly due to drying the latter during sample preparation. T_{dehydr} was highest (83 °C) for the untreated powder and showed a moderate shift towards lower values for the control (77 °C) and heat-treated (75 °C) samples, indicating somehow weakened protein-water interactions, at the higher moisture content of the former. At T > 175 °C, evolved gases for the three samples showed the characteristic FTIR peaks for NH_3 (750–1250 cm^{-1}, 1600–1650 cm^{-1}, 3310–3360 cm^{-1}) and CO_2 (2250–2400 cm^{-1}), the main products of protein degradation.

DSC curves showed similar T_{denat} for the three samples (121–129 °C). However, the enthalpy change of the heat-treated PPI was lower compared to the control and untreated PPI by 50% and 75%, respectively. This suggests that (i) even the mild treatment of dispersing in water and freeze-drying can affect how the proteins interact with water; and (ii) the proteins that unfolded during heat-treatment to 95 °C (reported T_{denat} 77 °C for pea protein [38], 88 °C for pea legumin [39]) may have changed conformation and remained partially unfolded during cooling, resulting in decreasing ΔH for the partially pre-denatured PPI. It is not clear why the denaturation ΔH of the control sample was lower than that of the untreated PPI. It may be related to the higher water content of the untreated sample compared to the control, which promotes denaturation during the DSC measurement. It is also possible that hydration may induce molecular

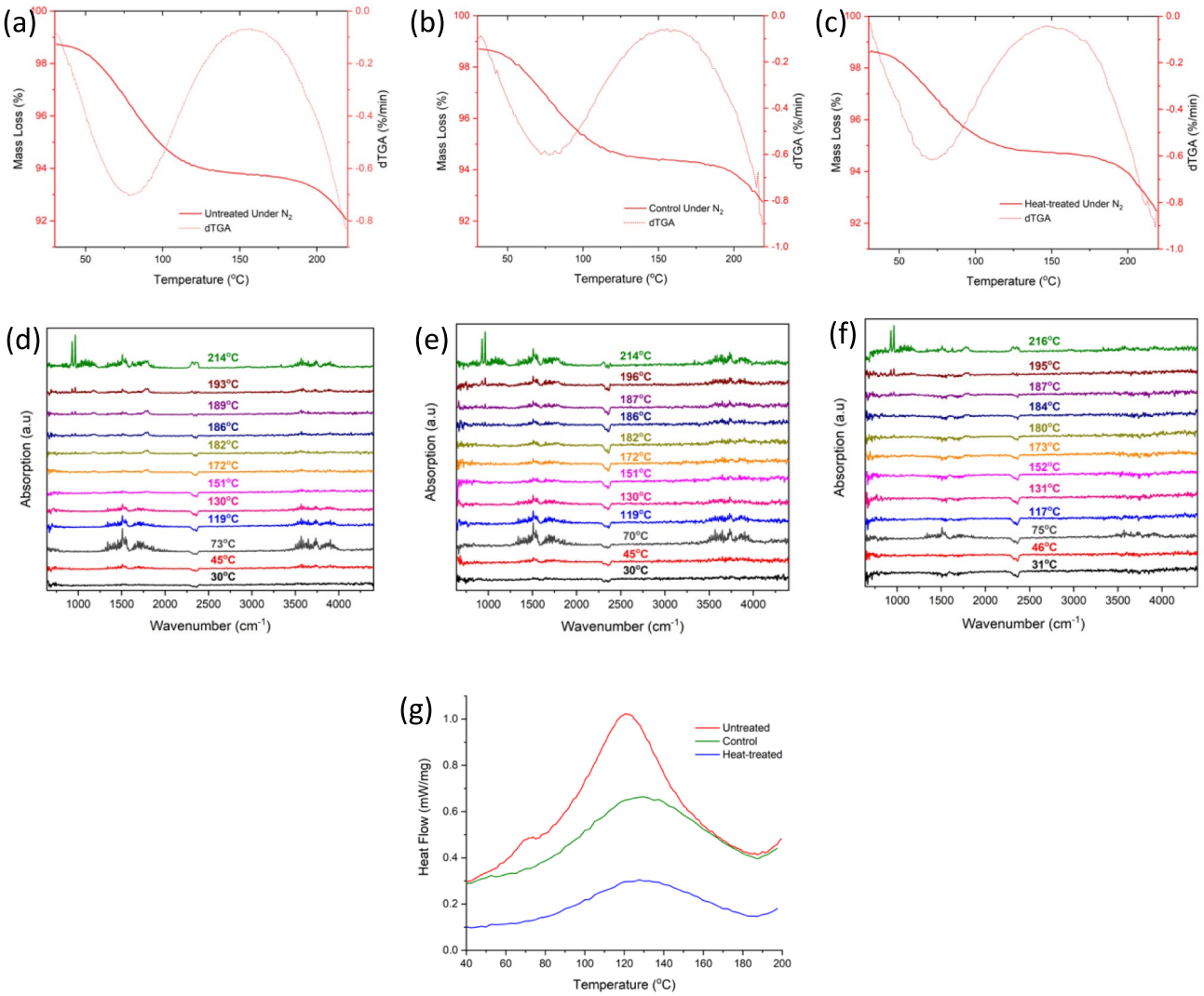

Fig. 4 Thermal analysis of the untreated, control, and heat-treated PPI showing the TGA curves under N_2 at heating rate 10 K/min (a: untreated; b: control; c: heat-treated), the related evolved gas FTIR spectra from the same experiments (d: untreated; e: control; f: heat-treated), and the DSC heating curves at 10 K/min (g)

Table 2 Summary of thermal properties of the untreated, control, and heat-treated PPI determined by TGA (mass loss at 170 °C, T_{dehydr}) and DSC (T_{denat}, ΔH) experiments

Sample	Mass loss (%)	T_{dehydr} (°C)	T_{denat} (°C)	ΔH (J/g)
Untreated	7.3	83	121	215
Control	5.8	77	129	112
Heat-treated	6.1	75	128	63

changes to the proteins, for example through the formation of a dynamic surface thin layer of hydrogen-bonded water [40], which may affect the small-scale motions of the molecule after drying, and result in the observed reduced ΔH. The presence of small, flexible peptides (with sequences of < 8 residues) that are reportedly found in PPI [41, 42] may further contribute to increased interactions with water during hydration and before drying, resulting in the observed changes at low temperatures.

The XRPD patterns of the three samples display the characteristic peaks for protein structures at 2θ around 9.5° and 20° (Fig. 5, Table 3), typical of α- helices and β-sheets, respectively [43], albeit the peak at 19.8° has also been previously related to amorphous protein regions for the 7S and the 11S soy legumins [44]. A peak at 31.7° was further observed for all samples, while the control and heat-treated samples exhibited an additional peak at 33.7°, which was not seen in the untreated PPI. The latter is attributed to the

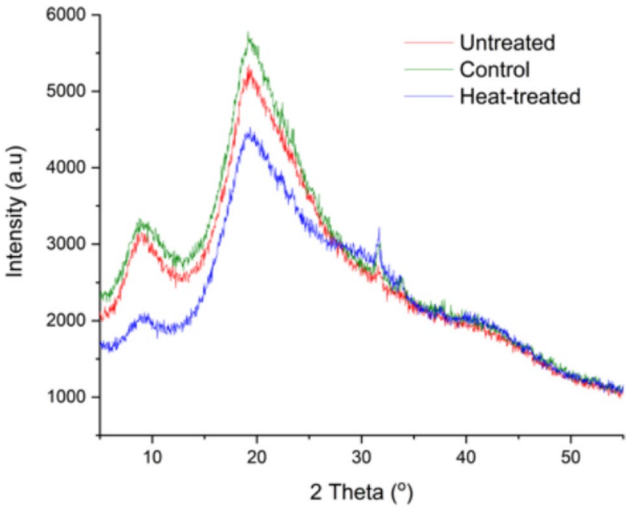

Fig. 5 X-Ray diffraction patterns for the untreated, control, and heat-treated PPI with 2θ from 5 to 55°

formation of new crystalline-like regions during PPI treatment. A similar peak at 33.7° has been previously attributed to new crystals formed during treatment of soy protein isolate with shellac [45]. The absence of a peak at 34.4° could indicate absence of cellulose and other lignocellulosic material in the PPI, as it has been previously reported [46]. While quantitative interpretation of the obtained powder patterns is challenging [47], Fig. 5 suggests that heating induced a shift towards less α-helices and more β-sheets, and an associated reduction in relative crystallinity, which has also been reported for grass pea proteins [43]. At a molecular level, β-sheets are known to be more flexible than α-helices, which has been associated with proteins that are more soluble, denature at higher temperatures, and show increased emulsifying properties, compared to those with higher content of α-helices [48, 49]. In the present work, the heat-treated, β-sheet-rich proteins showed increased solubility (Fig. 2) and emulsifying properties (Sect. "Effect of heat on emulsification and gelation of PPI."), but denaturation temperature was similar to the non-heated proteins (Table 2).

Overall, the results suggest that the heat-treated PPI is less crystalline and possibly molecularly more flexible (XRPD), likely partially denatured (DSC), slightly less thermostable (TGA-FTIR) and contains less confined water (TGA-FTIR), compared to the control.

Effect of Heat on Emulsification and Gelation of PPI.

Emulsion Stability

The ζ-potential of control and heat-treated emulsions (≈−45 meV, Table 4) indicated sufficiently charged oil drop surfaces to limit coalescence, as previously reported [50]. Compared to non-emulsified particles, the net charge increased after emulsification likely due to changes in protein conformation during adsorption, as the hydrophobic regions were directed towards the oil phase and the more charged, hydrophilic regions set on the surface [50]. The ζ-potential values in Table 4 are within the reported range for PPI dispersions (e.g., −33.0 mV [50]; −43.5 mV [51]).

Heating can reduce particle sizes through separating the weakly bound aggregates; or it may increase particle sizes through promoting formation of new aggregates as the proteins may denature, exposing previously hidden hydrophobic regions that adhere together. The degree of aggregation is often higher than that of breakage, for example particle size increase has been reported on heating of pea protein isolate [20] and concentrate [52]. However, in Table 4, heating reduced particle sizes compared to the control, particularly the Sauter mean diameter D_{32} by 90% in the emulsions (from 16 to 1.6 µm) and by 60% in the suspensions (from 78 to 30 µm). For protein particles, this is likely related to the extensive initial degree of aggregation and the selected

Table 4 ζ-potential and Sauter mean diameter (D_{32}) of control and heat-PPI before and after homogenisation (samples A and B in Fig. 1), and after emulsification with rapeseed oil (samples C)

Sample	Not homogenised	Homogenised	Emulsified
ζ-potential (mV)			
Control	$-40.0 \pm 1.5^{a*}$	-39.0 ± 0.4^{a}	-46.2 ± 0.6^{b}
Heated	-41.4 ± 1.5^{a}	-41.6 ± 0.4^{a}	-44.2 ± 1.1^{b}
Average particle size (D_{32}, µm)			
Control	78.2 ± 0.3^{a}	48.9 ± 1.4^{b}	15.9 ± 2.8^{c}
Heated	30.8 ± 2.7^{a}	19.5 ± 2.0^{b}	1.6 ± 0.1^{c}

*Significant differences are indicated for each sample (i.e., per row) with letter-case.

Table 3 Angle (2θ) and associated distances (d) of XRPD peaks, and total relative crystallinity of untreated, control, and heat-treated PPI. 2θ is given in degrees (°)

Sample	Peak 1		Peak 2		Peak 3		Peak 4		Rel. crystal. (%)
	2θ°	d (Å)	2θ°	d (Å)	2θ°	d (Å)	2θ°	d (Å)	
Untreated	9.01	9.80	19.28	4.60	31.69	2.82	n/a	n/a	37
Control	9.16	9.64	19.32	4.59	31.80	2.81	33.94	2.64	40
Heated	9.24	9.56	19.36	4.58	31.69	2.82	33.71	2.66	25

heating conditions, as aggregation could increase in longer heating times [20]. For oil droplets, reduced sizes may be related to the more soluble, smaller, and more flexible nature of the heat-treated proteins, compared to the control, that stabilise the oil fast during emulsification, thus limiting coalescence.

The heat-treated sample showed higher physical stability compared to the control. This is observed in Fig. 6, where after 7 days of storage, the control sample showed evident phase separation, with clear oil patches segregating from the matrix resulting in highly fluctuating backscattering values, compared to the heat-treated sample (blue lines in Figs. 6b and d). It is hypothesised that increased stability against coalescence was due to a more resistant interfacial film around the drops. The more soluble, partially denatured, less ordered, and more flexible nature of heat-treated proteins may facilitate fast adsorption and subsequent denaturation at the oil/water interface and formation of a stronger train-loop-tail conformation, effectively limiting coalescence [53]. Increased stability against coalescence for oil droplets stabilised by denatured proteins has previously been also attributed to increased protein-water interactions leading to higher degree of hydration of the interfacial film [54].

Reduced particle sizes in the heat-treated sample were further expected to increase stability against creaming, as smaller oil drops are known to rise slower compared to larger drops, in agreement to Stoke's law [55]. This has previously been reported for emulsions based on pea protein [20, 56], soy protein [19, 57], and egg yolk[55]. However, it was challenging to evaluate it in the present study due to the large number of air bubbles initially trapped into the bulk during emulsification, which travelled to the top during storage and masked creaming by forming a foam (Fig. 6). The foam was more stable for the heat-treated sample, as heating of the proteins resulted in more stable air bubbles, also previously observed [58]. A stable foam was evident for the heat-treated sample after 7 days of storage.

Structure and Rheological Properties of Emulsions and Gels

Microstructure of emulsions and gels was coarser for the control compared to the heat-treated systems (Fig. 7). CLSM images further suggest that oil droplets are surrounded (and likely stabilised) by proteins, as a layer of brown hue on the surface of the red-coloured oil drops indicates the presence of green-coloured protein particles. It is expected that protein molecules, unseen by CLSM but present in dynamic equilibrium with the particles [59], may also contribute to oil drop stabilisation. Macroscopically, the surface of the control gel appeared homogeneous (Figs. 7c and 7f). The gel prepared with heat-treated PPI had a wrinkled surface,

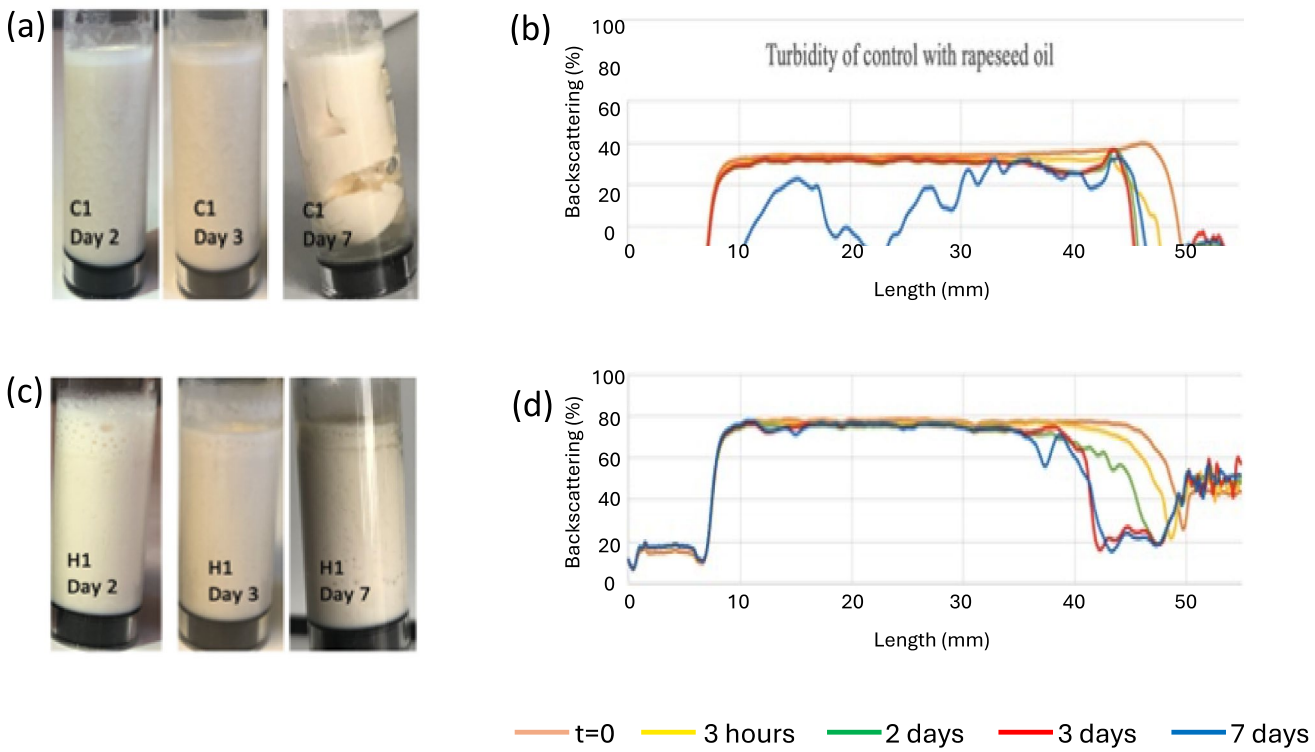

Fig. 6 Appearance (**a**, **c**) and backscattering (**b**, **d**) of emulsions prepared with the control (**a**, **b**) and heat-treated (**c**, **d**) PPI with time

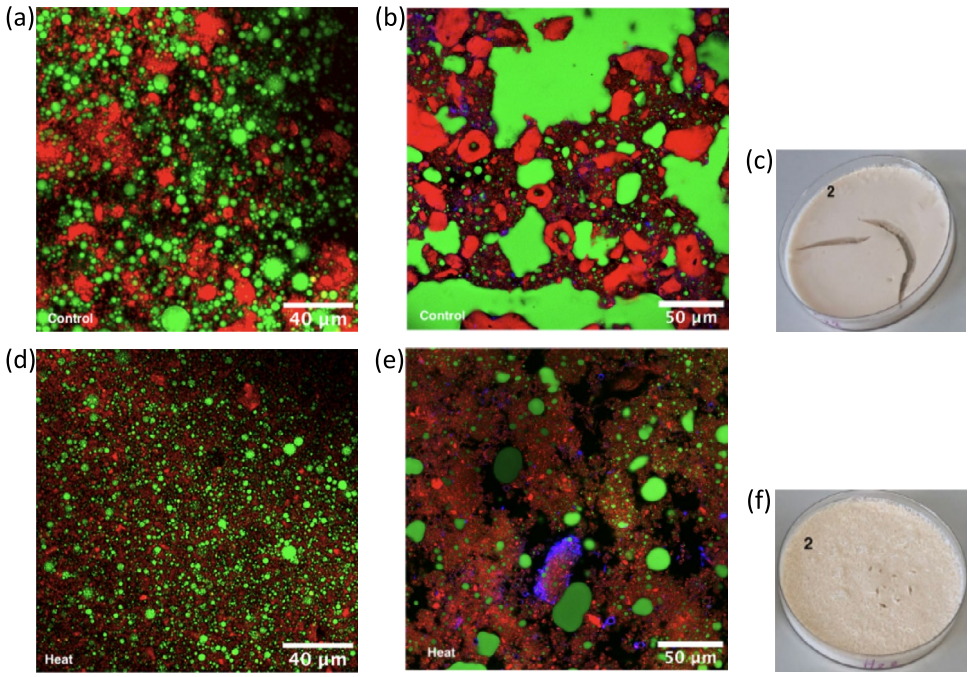

Fig. 7 Confocal laser scanning microscopy images of emulsions (**a**, **d**) and gels (**b**, **e**) prepared with control (**a**, **b**) and heat-treated (**d**, **e**) PPI; macroscopic pictures of the gels prepared with the control (**c**) and heat-treated (f) PPI. Lipids appear green, proteins red

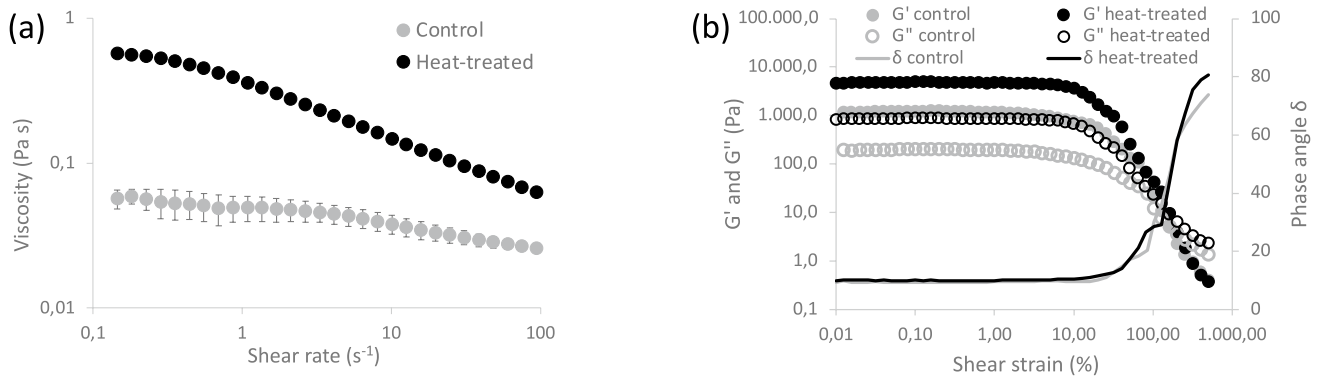

Fig. 8 Rheological properties of control (grey) and heat-treated (black) systems: (**a**) emulsion viscosity; (**b**) elastic (filled dots) and loss (empty dots) moduli and phase angle (line) of the gels

likely due to the presence of stable air bubbles that burst after the gel was set.

Emulsions prepared with heat-treated PPI showed higher viscosities and increased shear-thinning behaviour compared to the control (Fig. 8a, Table 5). Increased shear thinning is evidenced by a power-law index that is lower than 1. This is expected for systems with smaller drop sizes [31, 60, 61], compared to systems with coarser drops, due to the increased drop surface area and related particle–particle interactions that are high at low shear rates and decrease as shear rate increases, as the drops align themselves to the direction of the flow. Increased viscosity on decreasing oil drop size has previously been reported for PPI-based emulsions [62].

For both systems, gel-like character after acidification was confirmed as G' > G'' (Fig. 8b). The gel-like material prepared with the heat-treated PPI had higher moduli compared to the control, indicative of a stiffer hydrogel [63]. In addition, the linear viscoelastic region (LVR), defined as the region in the strain sweep test ending when G' loses 5% of its initial value, was greater for the heat-treated-PPI-based

Table 5 Power-law indices and consistencies (n and K in Eq. 2) of emulsion prepared with the control and heat-treated PPI

	Power-law index (n)	Consistency (Pa s^n)
Control	$0.88 \pm 0.02^{a*}$	0.048 ± 0.009^{a}
Heat-treated	0.64 ± 0.00^{b}	0.34 ± 0.01^{b}

*Significant differences are indicated for the n and K (i.e., per column) as letter-cases

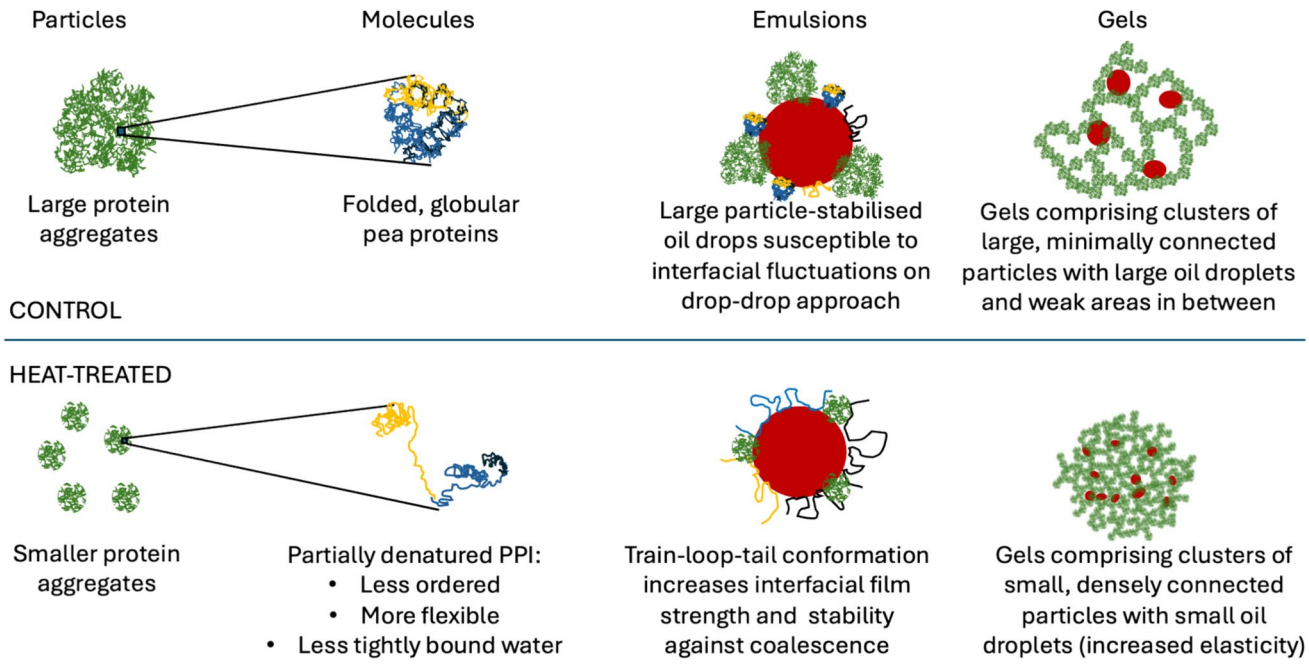

Fig. 9 Suggested mechanism of the effect of heat-treatment on PPI properties and resulting functionality (schematic). Protein particles are in green; protein subunits are in blue, black, and yellow; oil droplets are in red

gel compared to the control gel (ending at strains of 5% and 3%, respectively), indicating resistance to breakage, attributed to higher degree of particle–particle interactions [63]. This may be due to the more soluble, and less tightly-bound-to-water heat-treated protein particles and the smaller oil drop sizes, enhancing the number of possible interactions. Thermal treatment has been previously reported to increase elasticity of acid-induced gels from brewers' spent grain [26].

Conclusions

This work presents results on how heat-treatment may affect the physicochemical properties of PPI and associated functionality, with the aim to contribute towards a better understanding of the material and future design of plant-based foods with predictable attributes. Heat-treatment was found to affect protein particle size and molecular conformation. Heat-treated PPI particles were smaller, and contained proteins that were more soluble, less ordered, partially denatured, more flexible, and less tightly bound to water, compared to the control. These characteristics enhanced protein-oil interactions and produced more stable emulsions against coalescence and creaming. They also enhanced protein–protein interactions and produced more elastic gels. Suggested mechanisms are schematically summarised in Fig. 9.

Acknowledgements We thank the STFC Rutherford Appleton Laboratory for express access to the TOSCA beamline via beam time. The thermoanalysis instrument was financed by the Carlsberg Foundation (grants 2013_01_0589, CF14-0230, and CF20-0130). Confocal laser scanning microscopy images and XRPD data were acquired at the Center for Advanced Bioimaging (CAB) and the Department of Chemistry, respectively, at the University of Copenhagen, Denmark. Rui Liu and Heloisa N. Bordallo were supported by the Marie Skłodowska Curie EU's Horizon 2020 research and innovation programme [PICKFOOD grant number 956248]. Poul Erik Jensen and Ourania Gouseti wish to acknowledge funding from the Independent Research Fund Denmark projects 1127-00110B and 2101-00023B, respectively.

Author Contributions Serafim Bakalis, Poul Erik Jensen, Heloisa Nunes Bordallo, and Ourania Gouseti contributed to the study conception and design. Material preparation, data collection and analysis were performed by Rui Liu, Camilla Frederiksen, Trine Rasmussen, and Svemir Rudić. The first draft of the manuscript was written by Rui Liu, Camilla Frederiksen, Trine Rasmussen, and Ourania Gouseti and all authors commented on previous versions of the manuscript. All authors reviewed, read, and approved the final manuscript.

Funding Open access funding provided by Copenhagen University.

Data Availability Raw data are available on request.

Declarations

Conflict of Interest The authors declare no competing interests.

References

1. FAO Key Facts and Findings 6–6 (2019) https://doi.org/10.30875/e36cfd60-en
2. E.B. Richi, B. Baumer, B. Conrad, R. Darioli, A. Schmid, U. Keller, Health Risks Associated with Meat Consumption: A Review of Epidemiological Studies. Int. J. Vitam. Nutr. Res. **85**, 70–78 (2015)
3. R.E. Aluko, O.A. Mofolasayo, B.M. Watts, Emulsifying and Foaming Properties of Commercial Yellow Pea (Pisum Sativum L) Seed Flours. J Agric Food Chem **57**, 9793–9800 (2009). https://doi.org/10.1021/jf902199x
4. M. Barac, S. Cabrilo, M. Pesic, S. Stanojevic, S. Zilic, O. Macej, N. Ristic, Profile and Functional Properties of Seed Proteins from Six Pea (Pisum Sativum) Genotypes. Int J Mol Sci **11**, 4973–4990 (2010). https://doi.org/10.3390/ijms11124973
5. J. Rivera, K. Siliveru, Y. Li, A comprehensive review on pulse protein fractionation and extraction: Processes, Functionality, and Food Applications. Crit Rev Food Sci Nutr. (2022). https://doi.org/10.1080/10408398.2022.2139223
6. Y. Tao, Y. Chen, W. Howard, M. Ibrahim, S.M. Patel, W.P. McMahon, Y.J. Kim, J.A. Delmar, D. Davis, Mechanism of Insoluble Aggregate Formation in a Reconstituted Solution of Spray-Dried Protein Powder. Pharm Res **40**, 2355–2370 (2023). https://doi.org/10.1007/s11095-023-03524-x
7. O. Gouseti, M.E. Larsen, A. Amin, S. Bakalis, I.L. Petersen, R. Lametsch, P.E. Jensen, Applications of Enzyme Technology to Enhance Transition to Plant Proteins: A Review. Foods **12**, 2518 (2023). https://doi.org/10.3390/foods12132518
8. Yan, J.; Zhao, S.; Xu, X.; Liu, F. Enhancing Pea Protein Isolate Functionality: A Comparative Study of High-Pressure Homogenization, Ultrasonic Treatment, and Combined Processing Techniques. Curr. Res. Food Sci. **2024**, 8, https://doi.org/10.1016/j.crfs.2023.100653
9. Bhuiyan MHR, Yeasmen N, Ngadi M. Effect of Food Hydrocolloids on 3D Meat-Analog Printing and Deep-Fat-Frying. Food Hydrocoll. 159 (2025) https://doi.org/10.1016/j.foodhyd.2024.110716
10. Hafizur Rahman Bhuiyan M, Yeasmen N, Ngadi M. Restructuring Plant-Derived Composites towards the Production of Meat-Analog Based Coated Fried Food. Food. Chem. **443** (2024), https://doi.org/10.1016/j.foodchem.2024.138482
11. Bhuiyan, M.H.R.; Ngadi, M. Thermomechanical Transitions of Meat-Analog Based Fried Foods Batter Coating. Food Chem. **447** (2024) https://doi.org/10.1016/j.foodchem.2024.138953.
12. Bhuiyan MHR, Liu L, Samaranayaka A, Ngadi M Prediction of Pea Composites Physicochemical Traits and Techno-Functionalities Using FTIR Spectroscopy. LWT **208** (2024) https://doi.org/10.1016/j.lwt.2024.116667.
13. Bhuiyan MHR., Liu L, Samaranayaka A, Ngadi M Characterization of Pea Composites and Feasibility of Heat-Modulated Meat Analogs Production. Food Chem **463** (2025) https://doi.org/10.1016/j.foodchem.2024.141282
14. Y. Levy, J.N. Onuchic, Water and Proteins: A love-hate relationship. PNAS. **101**(10), 3325–3326 (2004). https://doi.org/10.1073/pnas.0400157101
15. Levine H, Slade, L. Water as a Plasticizer: Physico-chemical aspects of low-moisture polymeric systems. in Water Science Reviews 3, (Cambridge University Press, 2010), pp. 79–185. https://doi.org/10.1017/CBO9780511552083.002
16. Ruiz GN, Romanini M, Hauptmann A, Loerting T, Shalaev E, Tamarit JL, Pardo LC, Macovez, R. Genuine Antiplasticizing Effect of Water on a Glass-Former Drug. Sci. Rep. **7** (2017) https://doi.org/10.1038/s41598-017-07643-5
17. J. Flory, S. Alavi, Use of Hydration Properties of Proteins to Understand Their Functionality and Tailor Texture of Extruded Plant-Based Meat Analogues. J Food Sci **89**, 245–258 (2024). https://doi.org/10.1111/1750-3841.16804
18. Ma KK, Greis M, Lu J, Nolden AA, McClements, D.J.; Kinchla, A.J. Functional Performance of Plant Proteins. Foods **11** 2022
19. M. Keerati-u-rai, M. Corredig, Heat-Induced Changes in Oil-in-Water Emulsions Stabilized with Soy Protein Isolate. Food Hydrocoll **23**, 2141–2148 (2009). https://doi.org/10.1016/j.foodhyd.2009.05.010
20. W. Peng, X. Kong, Y. Chen, C. Zhang, Y. Yang, Y. Hua, Effects of Heat Treatment on the Emulsifying Properties of Pea Proteins. Food Hydrocoll **52**, 301–310 (2016). https://doi.org/10.1016/j.foodhyd.2015.06.025
21. R. Andoyo, A.Z. Diani, F. Fetriyuna, Effect of heating temperature on physical, functional, and digestibility properties of whey protein concentrate (WPC). in Proceedings of the IOP Conference Series, Earth and Environmental Science, Institute of Physics. **1230** (2023). https://doi.org/10.1088/1755-1315/1230/1/012155
22. E. Foegeding Allen, J.P. Davis, Food Protein Functionality: A Comprehensive Approach. Food Hydrocoll **25**, 1853–1864 (2011)
23. Shen Y, Du Z, Wu X, Li Y Modulating Molecular Interactions in Pea Protein to Improve Its Functional Properties. J Agric Food Res **8** (2022) https://doi.org/10.1016/j.jafr.2022.100313.
24. A. Lopez-Rubio, E.P. Gilbert, Neutron Scattering: A Natural Tool for Food Science and Technology Research. Trends Food Sci. Technol. **20**, 576–586 (2009)
25. M.M. Castellanos, A. McAuley, J.E. Curtis, Investigating Structure and Dynamics of Proteins in Amorphous Phases Using Neutron Scattering. Comput Struct Biotechnol J **15**, 117–130 (2017)
26. Hellebois T, Gaiani C, Planchon S, Renaut J, Soukoulis, C. Impact of Heat Treatment on the Acid Induced Gelation of Brewers' Spent Grain Protein Isolate. Food Hydrocoll. **113** (2021) https://doi.org/10.1016/j.foodhyd.2020.106531
27. L.P. Kirazov, L.G. Venkov, E.P. Kirazov, Comparison of the Lowry and the Bradford Protein as Applied for Protein Estimation o Membrane-Containing Fractions. Anal Biochem **208**, 44–48 (1993)
28. R.S. Pinna, S. Rudić, S.F. Parker, J. Armstrong, M. Zanetti, G. Škoro, S.P. Waller, D. Zacek, C.A. Smith, M.J. Capstick et al., The Neutron Guide Upgrade of the TOSCA Spectrometer. Nucl Instrum Methods Phys Res A **896**, 68–74 (2018). https://doi.org/10.1016/j.nima.2018.04.009
29. O. Arnold, J.C. Bilheux, J.M. Borreguero, A. Buts, S.I. Campbell, L. Chapon, M. Doucet, N. Draper, R. Ferraz Leal, M.A. Gigg et al., Mantid - Data Analysis and Visualization Package for Neutron Scattering and μ SR Experiments. Nucl Instrum Methods Phys Res A **764**, 156–166 (2014). https://doi.org/10.1016/j.nima.2014.07.029
30. C. Masiá, P.E. Jensen, I.L. Petersen, P. Buldo, Design of a functional pea protein matrix for fermented plant-based Cheese. Foods. **11**(2), 178 (2022). https://doi.org/10.3390/foods11020178
31. Barnes HA, Hutton JF, Walters K An Introduction to Rheology; Elsevier ltd. UK (1989)
32. M. Lassen, R. Bruenig, T.P. Czaja, A. Amin, K.E. Ørskov, T. Hannibal, L.B. Christensen, P.E. Jensen, O. Gouseti, Composite Starch/Fermented Protein Emulsion Gels for Plant-Based Cheese Applications. LWT **212**, 116863 (2024). https://doi.org/10.1016/j.lwt.2024.116863

33. M. Hishida, A. Kaneko, Y. Yamamura, K. Saito, Contrasting Changes in Strongly and Weakly Bound Hydration Water of a Protein upon Denaturation. J Phys Chem B **127**, 6296–6305 (2023). https://doi.org/10.1021/acs.jpcb.3c02970
34. Phan-Xuan, T.; Bogdanova, E.; Sommertune, J.; Fureby, A.M.; Fransson, J.; Terry, A.E.; Kocherbitov, V. The Role of Water in the Reversibility of Thermal Denaturation of Lysozyme in Solid and Liquid States. Biochem. Biophys. Rep. **28** (2021) https://doi.org/10.1016/j.bbrep.2021.101184
35. N. Kitabatake, M. Tahara, E. Dol, Thermal Denaturation of Soybean Protein at Low Water Contents. Agric Biol Chem **54**, 2205–2212 (1990). https://doi.org/10.1080/00021369.1990.10870318
36. L.J. Mauer, D.E. Smith, T.P. Labuza, Effect of Water Content, Temperature and Storage on the Glass Transition, Moisture Sorption Characteristics and Stickiness of β-Casein. Int J Food Prop **3**, 233–248 (2000). https://doi.org/10.1080/10942910009524630
37. Xiang L, Zhu W, Jiang B, Chen J, Zhou L, Zhong F Volatile Compounds Analysis and Biodegradation Strategy of Beany Flavor in Pea Protein. Food Chem **402** (2023) https://doi.org/10.1016/j.foodchem.2022.134275
38. J.L. Mession, M.L. Chihi, N. Sok, R. Saurel, Effect of Globular Pea Proteins Fractionation on Their Heat-Induced Aggregation and Acid Cold-Set Gelation. Food Hydrocoll **46**, 233–243 (2015). https://doi.org/10.1016/j.foodhyd.2014.11.025
39. F.E. O'Kane, R.P. Happe, J.M. Vereijken, H. Gruppen, M.A.J.S. Van Boekel, Heat-Induced Gelation of Pea Legumin: Comparison with Soybean Glycinin. J Agric Food Chem **52**, 5071–5078 (2004). https://doi.org/10.1021/jf035215h
40. R. Gazi, S. Maity, M. Jana, Conformational features and hydration dynamics of proteins in cosolvents: A perspective from computational approaches. ACS Omega **8**(3), 2832–2843 (2022). https://doi.org/10.1021/acsomega.2c08009
41. A. Cosson, L. Oliveira Correia, N. Descamps, A. Saint-Eve, I. Souchon, Identification and characterization of the main peptides in pea protein isolates using ultra high-performance liquid chromatography coupled with mass spectrometry and bioinformatics tools. Food Chem **367**, 130747 (2022). https://doi.org/10.1016/j.foodchem.2021.130747
42. A. Cosson, D. Blumenthal, N. Descamps, I. Souchon, A. Saint-Eve, Using a Mixture Design and Fraction-Based Formulation to Better Understand Perceptions of Plant-Protein-Based Solutions. Food Res Int **141**, 110151 (2021). https://doi.org/10.1016/j.foodres.2021.110151
43. M. Ghobadi, M.J. Varidi, A. Koocheki, M. Varidi, Effect of Heat Treatment on the Structure and Stability of Grass Pea (Lathyrus Sativus) Protein Isolate/Alyssum Homolocarpum Seed Gum Nanoparticles. Int J Biol Macromol **182**, 26–36 (2021). https://doi.org/10.1016/j.ijbiomac.2021.03.170
44. Li, C.; Tian, Y.; Liu, C.; Dou, Z.; Diao, J. Effects of Heat Treatment on the Structural and Functional Properties of Phaseolus Vulgaris L. Protein. Foods **12** (2023) 10.3390/foods12152869
45. Zhang Y, Li T, Zhang H, Zhang H, Chi Y, Zhao X, Li H, Wen Y Blending with Shellac to Improve Water Resistance of Soybean Protein Isolate Film. J Food Process Eng **43** (2020) https://doi.org/10.1111/jfpe.13515
46. Z. He, H.N. Cheng, O.M. Olanya, J. Uknalis, X. Zhang, B.D. Koplitz, J. He, Surface Characterization of Cottonseed Meal Products by SEM, SEM-EDS, XRD and XPS Analysis. J Mater Sci Res **7**, 28 (2017). https://doi.org/10.5539/jmsr.v7n1p28
47. G.M. Kavanagh, A.H. Clark, S.B. Ross-Murphy, Heat-induced gelation of globular proteins: Part 3. Molecular studies on low ph b-lactoglobulin gels; **28**(1), 41–50 (2000). https://doi.org/10.1016/S0141-8130(00)00144-6
48. K. Shevkani, N. Singh, Y. Chen, A. Kaur, L. Yu, Pulse proteins: Secondary structure, functionality and applications. J. Food. Sci. Technol. **56**, 2787–2798 (2019). https://doi.org/10.1007/s13197-019-03723-8
49. Yan S, Xu J, Zhang S, Li, Y. Effects of Flexibility and Surface Hydrophobicity on Emulsifying Properties: Ultrasound-Treated Soybean Protein Isolate. LWT **142** (2021) https://doi.org/10.1016/j.lwt.2021.110881
50. F. Keivaninahr, P. Gadkari, K. Zoroufchi Benis, M. Tulbek, S. Ghosh, Prediction of Emulsification Behaviour of Pea and Faba Bean Protein Concentrates and Isolates from Structure-Functionality Analysis. RSC Adv. **11**, 12117–12135 (2021). https://doi.org/10.1039/d0ra09302e
51. K. Shevkani, N. Singh, A. Kaur, J.C. Rana, Structural and Functional Characterization of Kidney Bean and Field Pea Protein Isolates: A Comparative Study. Food Hydrocoll **43**, 679–689 (2015). https://doi.org/10.1016/j.foodhyd.2014.07.024
52. Asen ND, Aluko R.E. Effect of Heat Treatment on Yellow Field Pea (Pisum Sativum) Protein Concentrate Coupled with Membrane Ultrafiltration on Emulsification Properties of the Isolated >50 KDa Proteins. Membranes (Basel) **13** (2023) https://doi.org/10.3390/membranes13090767
53. Kleshchanok, D.; Tuinier, R.; Lang, P.R. Direct Measurements of Polymer-Induced Forces. J Phys Condensed Matter **20** (2008) https://doi.org/10.1088/0953-8984/20/7/073101.
54. Palazolo GG, Sorgentini DA, Wagner, J.R. Coalescence and Flocculation in o/w Emulsions of Native and Denatured Whey Soy Proteins in Comparison with Soy Protein Isolates. In Proceedings of the Food Hydrocolloids; Elsevier, 2005; Vol. 19, pp. 595–604
55 F. Guilmineau, U. Kulozik, Impact of a Thermal Treatment on the Emulsifying Properties of Egg Yolk Part 2: Effect of the Environmental Conditions. Food Hydrocoll **20**, 1114–1123 (2006). https://doi.org/10.1016/j.foodhyd.2005.12.006
56. M. Chen, J. Lu, F. Liu, J. Nsor-Atindana, F. Xu, H.D. Goff, J. Ma, F. Zhong, Study on the Emulsifying Stability and Interfacial Adsorption of Pea Proteins. Food Hydrocoll **88**, 247–255 (2019). https://doi.org/10.1016/j.foodhyd.2018.09.003
57. Y. Shao, C.H. Tang, Characteristics and Oxidative Stability of Soy Protein-Stabilized Oil-in-Water Emulsions: Influence of Ionic Strength and Heat Pretreatment. Food Hydrocoll **37**, 149–158 (2014). https://doi.org/10.1016/j.foodhyd.2013.10.030
58. P. Moll, H. Salminen, E. Griesshaber, C. Schmitt, J. Weiss, Homogenization Improves Foaming Properties of Insoluble Pea Proteins. J. Food Sci. **87**, 4622–4635 (2022). https://doi.org/10.1111/1750-3841.16320
59. S. Sridharan, M.B.J. Meinders, J.H. Bitter, C.V. Nikiforidis, On the Emulsifying Properties of Self-Assembled Pea Protein Particles. Langmuir **36**, 12221–12229 (2020). https://doi.org/10.1021/acs.langmuir.0c01955
60. U. Teipel, Influence of Droplet Size on the Rheological Behavior of Emulsions. Chem. Eng. Technol. **25**, 609 (2002). https://doi.org/10.1002/1521-4125(200206)25:6%3c609::AID-CEAT609%3e3.0.CO;2-H
61. R. Pal, Effect of Droplet Size on the Rheology of Emulsions. AIChE J. **42**, 3181–3190 (1996). https://doi.org/10.1002/aic.690421119
62. N.A. McCarthy, D. Kennedy, S.A. Hogan, P.M. Kelly, K. Thapa, K.M. Murphy, M.A. Fenelon, Emulsification Properties of Pea Protein Isolate Using Homogenization. Microfluidization and Ultrasonication. Food Research International **89**, 415–421 (2016). https://doi.org/10.1016/j.foodres.2016.07.024
63. G. Stojkov, Z. Niyazov, F. Picchioni, R.K. Bose, Relationship between structure and rheology of hydrogels for various applications. Gels **7**(4), 255 (2021). https://doi.org/10.3390/gels7040255